Solar Cycle Effects on the Upper Atmosphere: Implications for Satellite Drag

R. L. Walterscheid*
The Aerospace Corporation, Los Angeles, California

High thermospheric temperatures are maintained against thermal diffusion primarily by the absorption of extreme ultraviolet (EUV) radiation by atmospheric constituents (mainly, atomic oxygen). Because the solar flux of EUV varies strongly over the 11-yr solar cycle, thermospheric temperatures likewise vary strongly over the solar cycle. In an average solar cycle, solar EUV and thermospheric temperature increase by about a factor of two from solar cycle minimum to solar cycle maximum. Because density is mainly an integrated effect of temperature, the change in density over the solar cycle is amplified with respect to the temperature change. Changes in temperature cause changes in composition and these changes act to mitigate the direct thermal effects. The net effect of temperature and composition is to give order-of-magnitude changes in density over the solar cycle. The atmospheric drag on satellites is proportional to atmospheric density. The effects on satellite lifetimes are profound. A fairly typical satellite initially at 500 km would have a lifetime of about 30 years under typical solar cycle minimum conditions and only about 3 years under solar maximum conditions. Large increases in the rate of change of orbital period from solar minimum to solar maximum are possible. The fractional increase in the highly reactive species atomic oxygen can exceed two orders of magnitude.

Nomenclature

a = radial distance from center of Earth to satellite
A = area-to-mass ratio
A_p = index of geomagnetic activity
C_D = drag coefficient
F_D = acceleration per unit mass due to drag
$F_{10.7}$ = index of solar 10.7 radio flux
g = acceleration due to gravity
H = pressure scale height [Eq. (6)]
H_i = scale height of ith constituent
H_0 = scale height at solar minimum
I = height-integrated effect of T/m [Eq. (13c)]
L = local effect of T/m [Eq. (13a)]
m = mean molecular weight
m_i = molecular weight of ith constituent
m_0 = mean molecular weight at solar minimum ($F_{10.7} = 75$)
n_i = number density of ith constituent
N = number of scale heights
P = atmosphere pressure
P_i = partial pressure of ith constituent
r = ratio of mass density for $Ap = 100$ to mass density for $Ap = 4$
R = gas constant of air (R^*/m)
R_0 = R at solar minimum ($F_{10.7} = 75$)
R^* = universal gas constant
t = time
t_L = satellite lifetime
$t_L(0)$ = satellite lifetime at solar minimum conditions
T = air temperature
T' = virtual temperature [Eq. (9)]
V = wind speed
$\mathbf{V}$ = wind vector
V_r = magnitude of $\mathbf{V}_r$
$\mathbf{V}_r$ = velocity of satellite with respect to the wind vector
V_s = magnitude of $\mathbf{V}_s$
$\mathbf{V}_s$ = satellite velocity in a corotating frame
z = altitude
z_0 = altitude where solar cycle variations are negligible
ρ = total mass density of air
ρ_i = mass density of ith constituent
ρ_0 = total mass density of air at solar minimum ($F_{10.7} = 75$)
μ = mass of Earth times gravitational constant
τ = orbital period
ω_s = angular orbital speed of satellite

Received Jan. 19, 1989; presented at the AIAA Aerospace Engineering Conference and Show, Los Angeles, CA, Feb. 14-16, 1989; revision received March 31, 1989.

*Research Scientist, Atmospheric Sciences Department, Space Sciences Laboratory.

I. Introduction

UNLIKE in the troposphere, where solar cycle effects are subtle, solar cycle effects in the thermosphere are profound. This is because the lower atmosphere responds to wavelengths of solar radiation that have a weak solar cycle dependence, while the thermosphere responds to wavelengths that have a very strong dependence. As a result of the solar cycle variation in the amount of solar radiation absorbed in the thermosphere, the thermosphere exhibits large solar cycle variations in temperature, density, composition, and winds.

The state of the thermosphere is also influenced by magnetospheric and ionospheric processes, which also have a solar cycle dependence. However, magnetospheric and ionospheric processes have their greatest influence at high latitudes, and on a global basis are less important than radiative processes.

The drag (deceleration) that satellites experience due to motion relative to the bulk motion of the atmosphere is

$$F_D = \tfrac{1}{2} C_D A \rho V_r^2 \tag{1}$$

$$\mathbf{V}_r = \mathbf{V}_s - \mathbf{V} \tag{2}$$

For given orbital parameters, F_D varies strongly over a solar cycle, and from one solar cycle to another. This is because F_D is proportional to ρ, and ρ exhibits large changes within and

between solar cycles. Above ~ 300 km, ρ at a given point can vary by an order of magnitude due to solar cycle variations. The dependence of F_D on V is weak because $V_s \gg V$. It is doubtful that solar cycle variations in F_D due to variations in V exceed a few percent. There are also solar cycle variations in C_D because C_D depends on composition and temperature.[1-3] However, variations in C_D are not large and are apt to be similar in significance to variations in V. This means that solar cycle changes in density are much more significant than changes in V and C_D.

The results presented in this paper are relevant for satellites in low Earth orbit (LEO) below ~ 800 km where drag effects are apt to be most important. In the following sections, solar cycle variations in density are discussed, including density variations caused by changes in the flux of extreme ultraviolet (EUV) radiation. The effects of solar cycle variations in magnetospheric and ionospheric processes are also briefly discussed.

Mechanisms of Density Change

The total mass density of a mixture of gases in given by

$$\rho = \frac{P}{(R^*/m)T} \tag{3}$$

and

$$m = \Sigma n_i m_i / \Sigma n_i \tag{4}$$

On average, the atmosphere is very nearly in hydrostatic balance. Applying this balance, one obtains the well-known hypsometric relation:

$$P = P(z_0) \exp\left(-\int_{z_0}^{z} \frac{dz'}{H} \right) \tag{5}$$

where

$$H = \frac{R^* T}{mg} \tag{6}$$

The quantity z_0 is chosen to be low enough that solar cycle variations are small.

Using Eq. (5) in Eq. (3) gives

$$\rho(z) = \frac{P(z_0)}{gH} \exp\left(-\int_{z_0}^{z} \frac{dz'}{H(z')} \right) \tag{7}$$

Thus, density at z is a function of the local and integrated values of temperature and composition. Note that the ideal gas law is $\rho = Pm/R^*T = P/gH$. Thus, the integrated effect is just $P/P(z_0)$. Generally, the integrated effects of temperature and composition dominate. This is borne out by the well-established fact that thermospheric ρ increases as T increases.

Physically, an increase in H causes an increase in pressure because less mass is traversed in going from the reference altitude z_0 to some other higher altitude z. Pressure is just the weight of the atmosphere per unit area above a given point. The smaller the amount of mass traversed in going from z_0 to z, the less weight per unit area one must subtract from the pressure at the reference altitude z_0 to obtain the pressure at z. In descriptive terms, pressure surfaces swell upward, and as a result a given pressure is found at greater heights.

To a first approximation, the thermosphere above ~ 110 km is in static equilibrium with each constituent distributed according to its own scale height.[4] Thus,

$$\rho_i(z) = \frac{P_i(z_0)}{gH_i} \exp\left(-\int_{z_0}^{z} \frac{dz'}{H_i} \right) \tag{8}$$

where

$$H_i = \frac{R^* T}{m_i g}$$

and the subscript i denotes values for the ith species. We have made the conventional assumption that all constituents have the same temperature.[4]

From the scale-height dependence exhibited in Eq. (8), it is obvious that each constituent will respond differently to a change in temperature. This implies that a change in thermospheric temperature will cause a change in composition, i.e., a change in mean molecular weight. Equation (7) implies that a change in thermospheric composition will affect total density.

The density response to a given change in thermospheric temperature is much weaker for constituents with long-scale heights such as helium than for constituents with short-scale heights such as argon. This is obvious from Eq. (8) since the integrand within the exponential is $1/H_i$. Figure 1 shows altitude profiles of helium and argon for $F_{10.7}$ ("solar max") over the equator. The profiles are predictions of the mass spectrometer incoherent scatter (MSIS) model[5] for day 80, local time 1500, and $Ap = 4$. Helium changes by an order of magnitude or less from solar minimum to solar maximum over the altitude range shown ($z \leq 800$ km), whereas argon changes by many orders of magnitude. Because heavier constituents respond more strongly to variations in thermospheric temperature than lighter ones, an increase in temperature results in an increase in the relative abundance of heavier constituents and the mean molecular weight increases. A decrease in thermospheric temperature, on the other hand, results in a decrease in mean molecular weight. According to Eq. (7), total density depends on the ratio T/m. Since m increases when T increases, and decreases when T decreases, the compositional effect mitigates the direct effect of temperature changes.

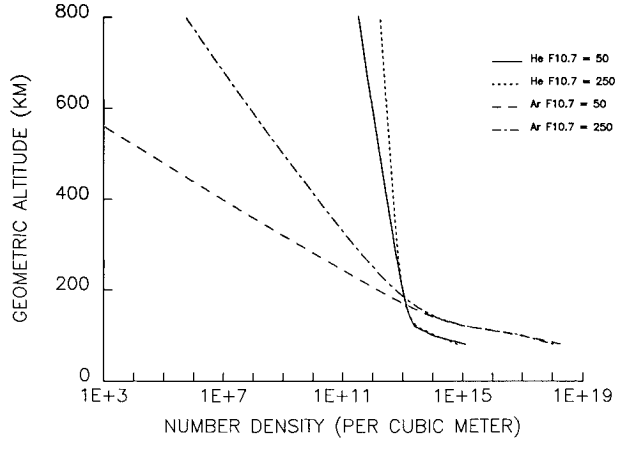

Fig. 1 Altitude profiles of argon and helium number densities at solar minimum and solar maximum.

Solar Cycle Variation in Solar EUV and Proxy Indices

As mentioned, solar cycle variations in total density are driven mainly by the heating of the global thermosphere by solar EUV radiation. This radiation dissociates and ionizes atmospheric constituents, the most important being oxygen. All of the incident EUV radiation is absorbed in the thermosphere, and after a complex set of processes ~ 20–30% of the incident energy goes into heating the thermosphere.[6]

Because none of the EUV radiation reaches the ground, the EUV variation cannot be monitored using ground-based techniques. Measurements of EUV have been made with rocket- and satellite-borne instruments, but these measurements are not made routinely, and continuous monitoring over an extended period of time has been limited to only a few satellite flights.[7] Observations are not sufficient to establish unequivocally the variability over the 11-yr cycle.[8]

Fortunately, proxy indices are available that are good indicators of the general level of solar activity and which can be

monitored continuously. Two indices that are in widespread use are the 10.7-cm solar flux ($F_{10.7}$) and the Zürich sunspot number R_z. Figures 2 and 3 show how these parameters correlate with EUV emissions, and some coronal emissions.[9] It is obvious that the $F_{10.7}$ and R_z indices correlate well with solar activity, and with each other. In the remainder of this paper, we will use the $F_{10.7}$ index to characterize the heating of the atmosphere by solar EUV.

Density Variations Over the Solar Cycle

In this section, results are presented for the solar cycle variation in density derived from the MSIS model.[10,11] The solar cycle is characterized in terms of the $F_{10.7}$ radio flux. The results refer to equatorial values at day 81, a local time of 1500, and a value of $Ap = 4$. Values of $F_{10.7}$ range from 75 to 200.

As discussed in an earlier section, density varies over the solar cycle as a result of variations in T and m. It is convenient to express these variations in terms of a single quality

$$T' = \frac{m_0}{m} T \tag{9}$$

where m_0 is the value of m at $F_{10.7} = 75$, which in this section is taken to be solar minimum. With this definition,

$$H = \frac{R^* T}{mg} = \frac{R^*}{m_0} \frac{T'}{g} = \frac{R_0 T'}{g} \tag{10}$$

and the variation of H over the solar cycle depends only on the variation of the virtual temperature T'.

Figure 4 shows the variation of T and T' over the solar cycle (i.e., over the range of $F_{10.7}$ values from 75 to 200). The left-hand scale is for altitudes of 400, 600, and 800 km. The right-hand scale is for an altitude of 200 km. We note a nearly linear relationship between temperature and solar flux at all altitudes. By 400 km, the thermosphere is essentially isothermal and this fact is reflected in the overlapping temperature curves for 400, 600, and 800 km.

The extent to which the T' curves deviate from the T curves is a measure of compositional effects. Compositional effects increase with altitude. At 200 km compositional effects are slight. However, by 600 km compositional effects have become quite significant. At this altitude, compositional effects cancel the effects of temperature so that the net effect of temperature and composition on density is small over the solar cycle. In fact, the initial effect of composition at low $F_{10.7}$ values is to effectively cool the thermosphere in terms of T'. At 800 km, this effective cooling is continued over the entire range of $F_{10.7}$ values and, by solar maximum, the effective cooling has become quite dramatic, the virtual temperature at solar maximum being ~ 450 K less than at solar minimum.

As mentioned previously, the density variation at a given altitude is the product of an integrated effect of temperature and composition and a local effect. Except at altitudes $\gtrsim 800$ km, these two effects oppose one another. The former is a consequence of hydrostatic balance and the dependence of density on pressure expressed by the ideal-gas law. The latter is just the consequence of the dependence on temperature and composition expressed by the ideal-gas law.

There is a tendency for the integrated effect to dominate owing to the exponential dependence on the integrated quantities. Generally, the variation in density will primarily reflect the net integrated effect of temperature and composition.

Because of the exponential dependence on the integrated effect of temperature, the density response to increased solar heating is much stronger than the temperature response. To see this, we form the ratio

$$\rho/\rho_0 = \frac{H_0}{H} \exp\left[\int_{z_0}^{z} \left(1 - \frac{H_0}{H}\right) \frac{dz}{H_0}\right] \tag{11}$$

Thus, a 10% increase in H gives

$$\frac{\rho}{\rho_0} \sim \frac{1}{1.1} e^{(0.1)(N)} \tag{12}$$

where N is the number of scale heights above z_0. For $N \sim 10$

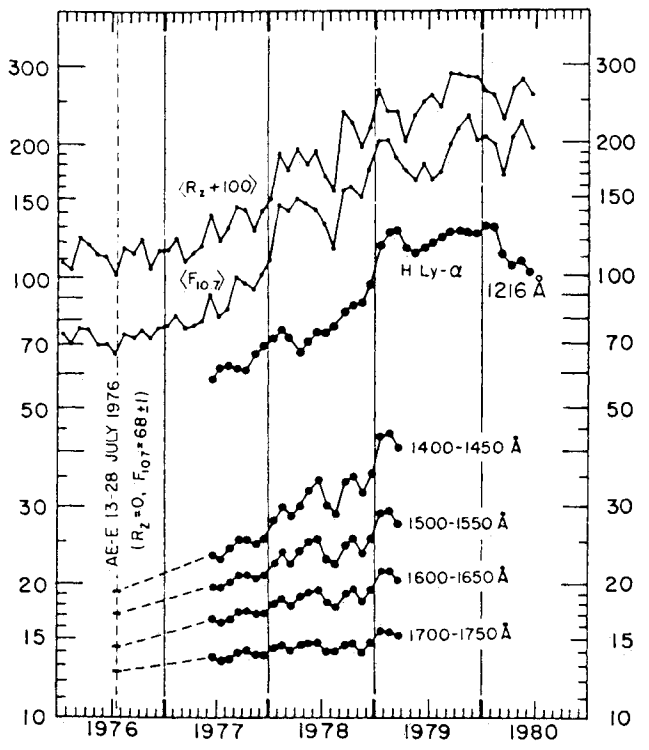

Fig. 2 Irradiance variations at wavelengths from 1216 to 1750 Å from AE-E satellite measurements during solar cycle 21.[9]

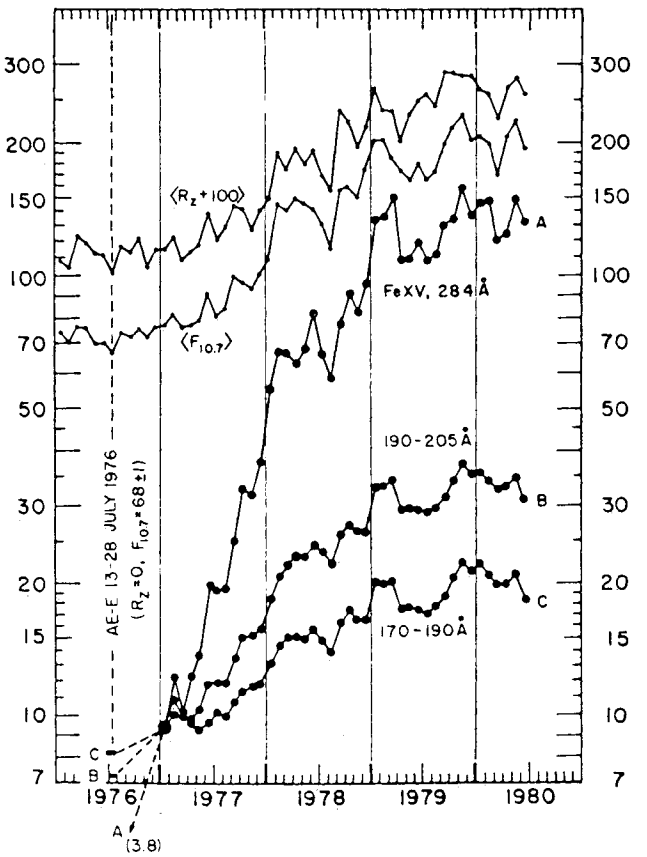

Fig. 3 Irradiance variations of some solar coronal emissions from AE-E satellite measurements during solar cycle 21.[9]

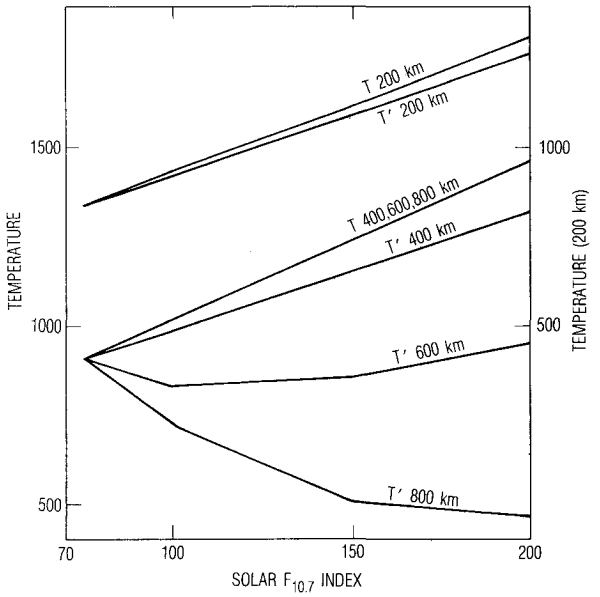

Fig. 4 Variation of T and T' vs solar flux as measured by the solar $F_{10.7}$ index.

(corresponding to an altitude of ~ 600 km), $\rho/\rho_0 \sim 3$, which is a factor of ~ 30 increase over the increase in scale height.

We now examine the solar cycle variation in density in terms of local L and integrated I effects at various altitudes. We write

$$\rho/\rho_0 = LI \tag{13a}$$

$$L = P/P_0 \tag{13b}$$

$$I = T_0/T' \tag{13c}$$

where the subscript 0 refer to solar cycle minimum conditions.

Figure 5a shows I for various altitudes as a function of solar flux. At all altitudes, I increases as the solar flux increases. The solar cycle increase is smallest at 200 km and largest at 600 km. This increase in I with altitude reflects the increasing number of scale heights covered by altitudes with T' increasing over the solar cycle. The altitude dependence of I changes sense somewhere above 600 km, and by the time 800 km is reached I is less than at 600 km. This is because of the compositional effects discussed earlier which result is a cooling of T' subsequent to solar minimum for altitudes $\gtrsim 600$ km. At altitudes where T' cools below its solar minimum value, the contribution to the integrand in Eq. (11) is negative and I decreases. Values of I at solar maximum range from 2.5 at 200 km to 21 at 600 km.

Figure 5b shows the same information for L as Fig. 5a showed for I. We note that whereas $I > 1$, L may contribute to an increase or decrease in density relative to solar minimum. The variation of L at 200 and 400 km is similar, with the local effect mitigating the integrated effect. At 600 km, the local effect is nil, whereas at 800 km it is significant and in the same sense as the integrated effect. This behavior is a direct reflection of the variation in T' shown in Fig. 4.

Figure 5c shows the product of L and I. Because the local effect is nil at 600 km, the net effect is the same as the integrated effect. Because the local effect at 800 km is large and in the same sense as the integrated effect, the combined effect causes the solar cycle variation at 800 km to be very similar to the variation at 600 km.

Geomagnetic Effects

The frequency of occurrence of magnetic storms has a solar cycle variation adapted from Hirman et al.[8] Figure 6 shows

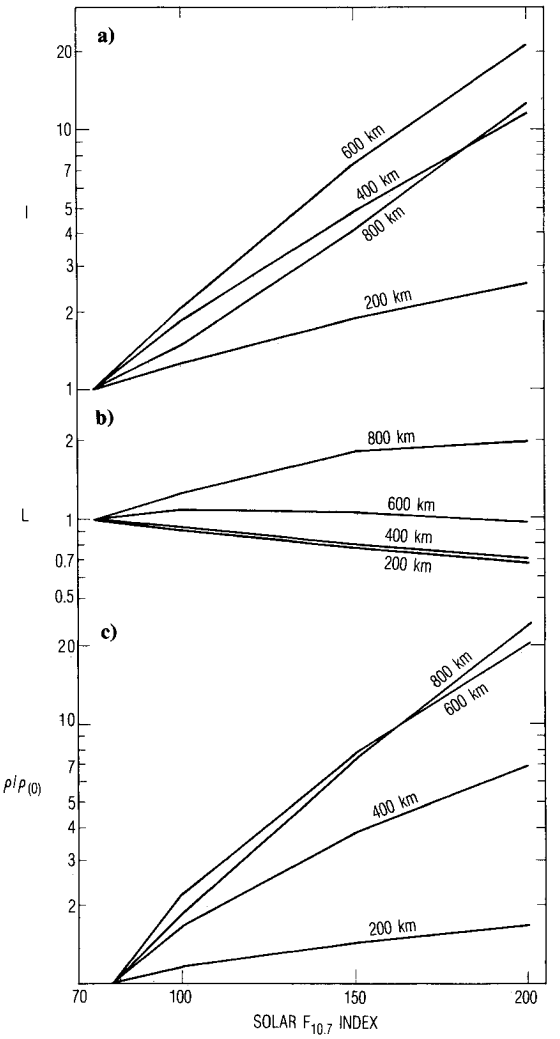

Fig. 5 a) Local and b) integrated contributions to the $\rho/\rho(0)$ vs $F_{10.7}$ index for various altitudes; c) variation of the ratio $\rho/\rho(0)$.

this variation for storms of various magnitudes. There is a pronounced maximum of magnetic-storm frequency during the declining phase of the solar cycle. Increased storm activity commences about halfway between solar maximum and solar minimum and persists to the beginning of the flat sunspot number variation defining solar minimum. There is a secondary maximum of shorter duration that ends near solar maximum.

Geomagnetic storms can cause intense warming of the polar cap and auroral regions by means of kinetic heating caused by the precipitation of energetic charged particles (mainly electrons) from the magnetosphere and Joule heating caused by the dissipation of electric fields originating in the magnetosphere. A global warming can result from the transport of heat by the large-scale wind system driven by the high-latitude heating.

Geomagnetic storms can cause large perturbations in thermospheric density. But these perturbations are comparatively short lived and are fairly infrequent. Major or severe storms are typically a few days to a week or so in duration and occur about twice monthly, on average, during the geomagnetically most active parts of the solar cycle. In addition, the total storm-energy input into the thermosphere over a solar cycle is certainly much less than the amount of EUV energy input attributable to solar cycle increases in the EUV flux over the flux at solar minimum.

Table 1 gives values of the ratio of density at moderately high geomagnetic activity ($Ap = 100$) to density at low activity ($Ap = 4$) predicted by the MSIS model.[10,11] Other fixed

parameters are $F_{10.7} = 100$, $LT = 15$ h, and day = 81. Values of $r \equiv \rho(Ap = 100)/\rho(Ap = 4)$ are tabulated for various altitudes and latitudes. Generally, r increases with increasing latitude and with increasing altitude. Values are an order of magnitude less than the values that are attributed to solar cycle variations and shown in Fig. 5.

As a consequence of the comparatively small changes in density and the limited duration and frequency of geomagnetic storms, solar cycle density variations caused by geomagnetic storms are of secondary importance with respect to satellite lifetime compared to variations caused by solar EUV heating.

The primary aerospace significance of geomagnetic storms is probably the consequences for the tracking required to maintain catalogs of Earth orbiting space objects. Tens of thousands of objects orbit the Earth, and discriminating objects of interest against a multitude of others requires precise predictions of satellite position. Perturbed conditions during geomagnetic storms can cause significant deviations from the expected positions, and result in satellites becoming lost.

Satellite Lifetimes

In this section, we present satellite-lifetime calculations. For convenience, we consider circular orbits and employ relations derived by King-Hele,[12] which account for the contraction of orbits.

The lifetime of satellites in circular orbits in given by King-Hele[12] as

$$t_L \cong \frac{-3H\tau}{2a\dot{\tau}} \tag{14}$$

where $\dot{\tau}$ is the time rate of change for the orbital period. The quantity τ is

$$\tau = \frac{2\pi a}{V_s} = \frac{2\pi}{\omega_s} \tag{15}$$

The quantity ω_s may be evaluated from the requirement for the centripetal acceleration to equal gravitational attraction, with the result

$$\omega_s^2 = \frac{\mu}{a^3} \tag{16}$$

Differentiating Eq. (15) and using Eq. (16) and Eq. (3.33) from Ref. 12 to evaluate $\dot{a}$ gives

$$\dot{\tau} = 3\pi a \rho C_D A \tag{17}$$

Equations (14) and (17) indicate that satellite lifetime is proportional to H/ρ. Using Eqs. (13), (14),and (17) gives the result

$$t_L/t_L(0) = L^{-2} I^{-1} \tag{18}$$

for a given initial orbit. According to Fig. 5, this means that the solar cycle variation of t_L at 200 km is slight, and the fractional decrease in t_L from solar minimum to solar maximum at 800 km is about half that at 600 km, despite the fact that the fractional density variations are similar at the two altitudes.

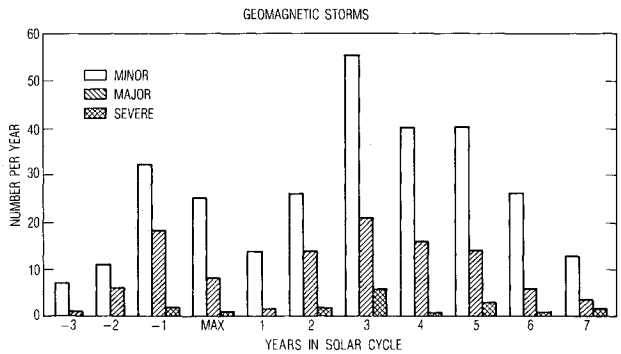

Fig. 6 Frequency of occurrence of geomagnetic storms of various magnitudes vs solar cycle.

Table 1 Variation of the ratio of density at $Ap = 100$ to $Ap = 4$ density vs altitude and latitude

	Latitude, deg north		
Altitude, km	90	45	0
200	1.57	1.32	1.27
400	1.92	1.60	1.66
600	2.55	2.26	1.82
800	2.38	2.04	1.83

Using Eqs. (14–17) and predictions of empirical models of atmospheric density, one can calculate t_L for various satellites. Figure 7 shows the results of calculations of t_L for a NASA Explorer-class satellite. Values of C_D and A are, respectively, 2.1 and 0.0027 kg m^{-2}. This satellite is a more or less typical compact high-density satellite. Results are given for values of $F_{10.7}$ from 75 to 250, and for initial satellite altitudes from 300 to 800 km. The calculations are based on MSIS-86.[5] Lifetimes are given along the ordinate. We note a very strong dependence of lifetime on altitude and $F_{10.7}$. There is roughly an order of magnitude decrease in t_L for a decrease in altitude of 100 km and for an increase in $F_{10.7}$ of 200 for altitudes above ~ 400 km. Below ~ 400 km, the dependence on $F_{10.7}$ is much less pronounced. This agrees with the data shown in Fig. 5.

Consider a satellite initially at 500 km. Under solar minimum conditions, the lifetime would be ~ 30 years, whereas under maximum condition the lifetime would be only ~ 3 years or less. We note that 30 years is much longer than a solar cycle. In practice, the lifetime would be somewhat longer than half a solar cycle depending on the launch date of the satellite.

Changes in Orbital Period

The changes in orbital period over time intervals of hours to days is of interest for satellite tracking and catalog maintenance. Equation (17) can be used to provide estimates of short-term changes in circular orbits.

Figure 8 gives the rate of the decrease in orbital period in seconds per day for the satellite and atmosphere model referred to in Fig. 7 (see previous section). The format is the same as for Fig. 7. In agreement with satellite lifetimes, the fractional changes relative to solar minimum increase with altitude. For an initial satellite altitude of 500 km, the relative change is a factor of ~ 30 from solar minimum to solar maximum. The largest absolute changes are at lower altitudes where drag is larger.

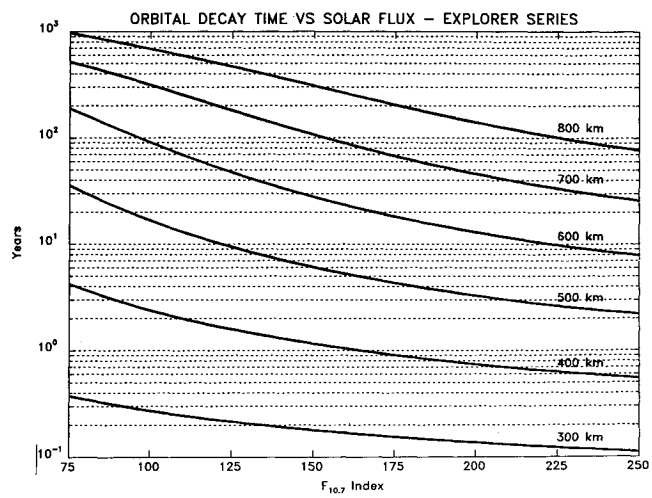

Fig. 7 Satellite lifetimes vs $F_{10.7}$ values for circular orbits for various initial altitudes.

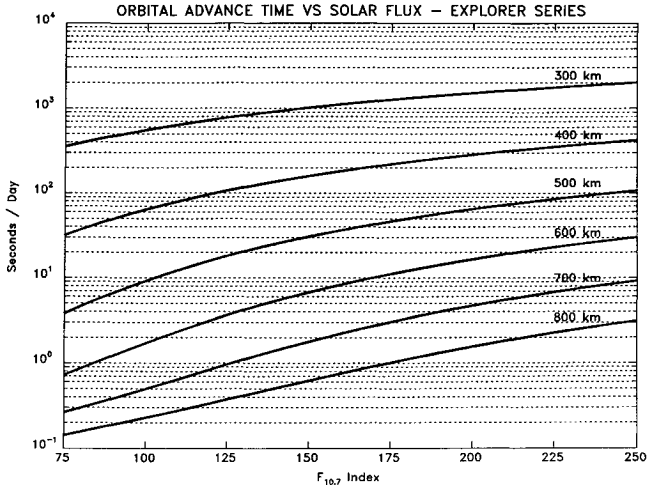

Fig. 8 Changes in orbital period vs $F_{10.7}$ values for circular orbit for various initial altitudes.

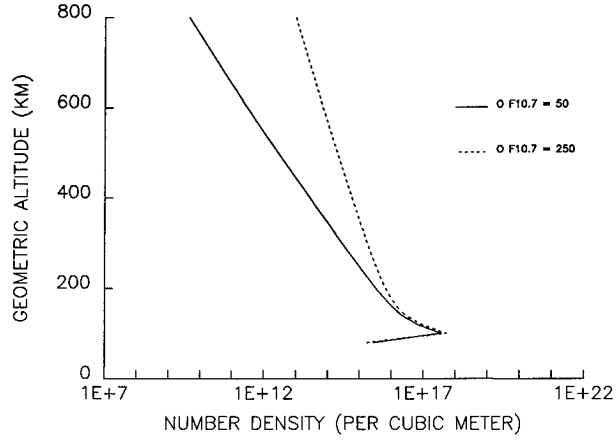

Fig. 9 Altitude profiles of atomic oxygen number density at solar minimum and solar maximum.

Atomic Oxygen Solar Cycle Variation

An important aspect of the solar cycle variation apart from drag is the variation in the highly reactive species, atomic oxygen. Atomic oxygen can react with thin organic films, advanced composites, and metallized surfaces[13] resulting in mass loss and degradation of sensor performance.

Above ~ 170 km, atomic oxygen is the most abundant species. At these altitudes, the fractional change in atomic oxygen number density over the solar cycle is similar to the fractional change in total density. Figure 9 shows altitude profiles of atomic oxygen number density over the equator for $F_{10.7}$ values of 50 (solar minimum) and 250 (solar maximum). These profiles are based on MSIS model[5] predictions for day 80, local time 1500, and $Ap = 4$. The solar cycle variation is small, up to ~ 150 km, but increases steadily and at the highest altitude shown (600 km) the atomic oxygen number density at solar maximum is several orders of magnitude greater than at solar minimum.

Conclusions

The major conclusions of this study, which apply to satellites in LEO $\lesssim$ 800 km, are given below:

1) Density changes over a solar cycle are the result of temperature changes and temperature-induced composition changes. Density changes occur because of changes in the ratio T/m.

2) Density changes locally because of both local and integrated changes in T/m. When solar cycle changes in T/m extend over a vertical layer more than a few scale heights in thickness, integrated effects dominate.

3) Above ~ 600 km, the ratio T/m decreases from its solar minimum values even though temperature is increasing.

4) The integrated effects of T/m dominate at all altitudes considered (200–800 km).

5) Below ~ 600 km, the local and integrated effects of T/m oppose each other, but above ~ 600 km they reinforce. Above ~ 600 km, order of magnitude changes in density occur from solar minimum to solar maximum.

6) The solar cycle variation of geomagnetic activity has comparative little effect on the long-term solar cycle variation in density, and is not a major influence on satellite lifetime. However, the short-term variation (day to weeks) may have important consequences for the tracking required to maintain a catalog of space objects.

7) Solar cycle variations in satellite lifetime reflect mainly solar cycle variations in density. The larger changes in density result in large changes in lifetimes. For a NASA Explorer-series satellite in a circular orbit at an initial altitude of 500 km, the lifetime varies from ~ 30 years at solar minimum to ~ 3 years at solar maximum for a more-or-less typical solar cycle.

8) During solar maximum, the concentration of the highly reactive species atomic oxygen can be enhanced over solar minimum concentrations by several orders of magnitude.

Acknowledgments

This work was supported by Aerospace Sponsored Research. I wish to thank Dr. D. Kayser from the Aerospace Corporation for helpful discussions and for providing Figs. 7 and 8, and Dr. M. Ross from the Aerospace Corporation for providing Figs. 3 and 9.

References

[1]Millikan, R. A., "The General Law of Fall of a Small Spherical Body Through a Gas and Its Bearing Upon the Nature of Molecular Reflection from Surfaces," *Physical Review,* Vol. 22, July 1923, pp. 1-23.

[2]Epstein, P. S., "On the Resistance Experienced by Spheres in Their Motion Through Gases," *Physical Review,* Vol. 23, June 1924, pp. 710-733.

[3]Schaaf, S. A. and Chambré, P. L., "Flow of Rarefied Gases," *Fundamentals of Gas Dynamics,* Vol. III, edited by H. W. Emmons, Princeton Univ. Press, Princeton, NJ, 1958, Sec. H, Chap. 2.

[4]Banks, P. M. and Kockarts, G., *Aeronomy,* Pt. A, Academic, New York, 1975.

[5]Hedin, A. E., "MSIS-86 Thermospheric Model," *Journal of Geophysical Research,* Vol. 92, May 1987, pp. 4649-4662.

[6]Torr, M. R., Richards, P. G., and Torr, D. G., "A New Determination of the Ultraviolet Heating Efficiency of the Thermosphere," *Journal of Geophysical Research,* Vol. 85, Dec. 1980, pp. 6819-6826.

[7]Hall, L. A., Heroux, L. J., and Hinteregger, H. E., "Solar Ultraviolet Irradiance," *Handbook of Geophysics and the Space Environment,* edited by A. S. Tursa, Air Force Geophysics Lab., 1985, Chap. 2.

[8]Hirman, J. W., Heckman, G. R., Greer, M. S., and Smith, J. B., "Solar and Geomagnetic Activity During Sunspot Cycle 21 and Implications for Cycle 22," *Transactions of the American Geophysical Society (EOS),* Vol. 69, Oct. 18, 1988, p. 962.

[9]Hinteregger, H. E., "AE-E Experiences of Irradiance Monitoring for 1250-1850 Å," *Proceedings of the Workshop on Solar UV Irradiance Monitors,* NOAA Environmental Research Lab., Boulder, CO, 1980.

[10]Hedin, A. E., Salah, J. E., Evans, J. V., Reber, C. A., Alcaydé, D., Bauer, P., Cogger, L., and McClure, J. P., "A Global Thermospheric Model Based on Mass Spectrometer and Incoherent Scatter Data. MSIS 1, N_2 Density and Temperature," *Journal of Geophysical Research,* Vol. 82, June 1977, pp. 2139-2147.

[11]Hedin, A. E., Reber, C. A., Newton, G. P., Spencer, N. W., Brinton, H. C., Mayr, H. G., and Potter, W. E., "A Global Thermospheric Model Based on Mass Spectrometer and Incoherent Scatter Data. MSIS 2, Composition," *Journal of Geophysical Research,* Vol. 82, June 1977, pp. 2148-2156.

[12]King-Hele, D., *Theory of Satellite Orbits in an Atmosphere,* Butterworths Mathematical Texts, London, 1964, Chaps. 3, 4.

[13]Visentine, J. T. (ed.), *Atomic Oxygen Effects Measurements for Shuttle Missions STS-8 and 41-G,* Vol. I-III, NASA TM-100459, Sept. 1988.